

# SIMULATION AND COMMISSIONING OF J-PARC LINAC USING THE IMPACT CODE

M. Ikegami, KEK, Tsukuba, Ibaraki 305-0801, Japan  
H. Sako, T. Morishita, JAEA, Tokai, Naka, Ibaraki 319-1195, Japan  
G. Shen, BNL, Upton, NY 11973-5000, USA

## Abstract

The IMPACT code has been utilized for the beam commissioning of J-PARC linac. The activity is presented by reviewing two illustrative topics, where the experimental data is analyzed to realize a finer tuning. One is the RF set-point tuning for a DTL tank, where we have a significant discrepancy between the experimental result and prediction from a simple numerical model. The other is the beam profile measurement, where significant beam quality deterioration is found to develop in a characteristic way. In both cases, the IMPACT code has helped us to deepen our insight into the beam behavior.

## INTRODUCTION

The beam commissioning of J-PARC linac was started in November 2006, and its initial stage was completed in October 2007 by achieving the linac beam power of 1.2 kW [1]. This beam power corresponds to 20 kW from the succeeding 3-GeV RCS (Rapid Cycling Synchrotron), and it is sufficient for the initial beam commissioning of the downstream facilities. Since then, J-PARC linac has been operated to provide a stable beam for the commissioning of downstream RCS, MR (Main Ring), and their beam lines to the experimental targets. After succeeding in delivering the first beams to all the experimental targets in May 2009, we are now in the next stage where we seek the operation with higher beam power.

J-PARC is a high-power frontier machine aiming at 1-MW beam power from RCS (133 kW from linac) in the final phase. Accordingly, it is of essential importance to reduce the uncontrolled beam loss, and hence, to avoid excess radio-activation of the accelerator components so as to maintain its hands-on maintenance capability. This is the case even in the early stages of the beam commissioning, and we need to reduce the integrated beam loss during the beam tuning. Therefore, it is required to realize a more sophisticated and efficient tuning rather than a traditional trial-and-error tuning. To this end, a simple and fast on-line numerical model plays an essential role in the beam commissioning of J-PARC linac.

On the other hand, the beams in a high-intensity linac are subject to strong space-charge forces. It often invokes collective and nonlinear phenomena, such as emittance growth and halo formation, being accompanied with the various operational errors. As these phenomena often lead to undesirable beam losses, we need to realize a precise tuning in

beam-power ramp-up. Even a very small fraction of beam loss can cause serious radio-activation in a high-intensity operation. Therefore, more thorough and fine-grained understanding of the beam behavior and the space-charge-driven phenomena is required in ramping up the beam intensity. To this end, we need a precise and detailed simulation of the beam behavior with a time-consuming PIC (Particle-In-Cell) tracking.

In the beam commissioning, we fully utilize two numerical models which complement each other. One is an on-line envelope model, and the other is an off-line PIC model.

As an on-line model, we have adopted XAL originally developed for SNS [2]. XAL is a JAVA-based high-level software development framework dedicated to accelerator beam commissioning, and it includes an envelope model to be utilized as an on-line model. This model is capable of calculating the evolution of rms beam widths and a beam center orbit swiftly. However, it can not simulate the space-charge-driven emittance growth and halo development. This model has been used for various beam tuning in J-PARC linac directly connected with high-level software [3].

As an off-line model, we have mainly adopted the IMPACT code developed at LBNL [4]. IMPACT is a fully three-dimensional PIC code optimized for parallel computing, which is suitable for the detailed simulation for the space-charge-driven phenomena including emittance growth, halo formation, and resulting beam loss. We use IMPACT for the beam simulation from the RFQ (Radio Frequency Quadrupole linac) exit to the injection point to RCS. The initial distribution for the IMPACT simulation is generated with the PARMTEQM code [5].

In this paper, we show some examples of the studies

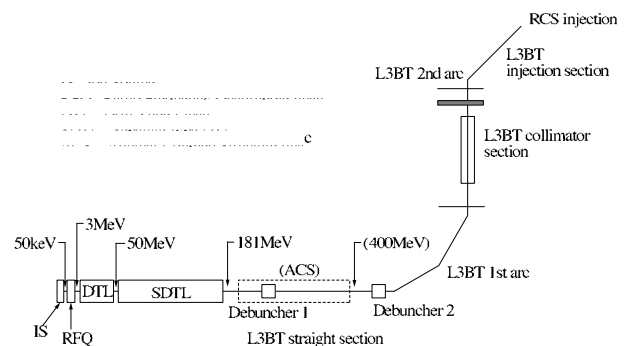


Figure 1: Schematic layout of J-PARC linac.

where the IMPACT code is used to analyze the experimental data obtained in the beam commissioning of J-PARC linac. In particular, we here take up the following two topics where the detailed simulation with the IMPACT code have helped us to deepen our understandings on the beam behavior in J-PARC linac. One is the phase-scan tuning of RF set-points for the first DTL tank (or DTL1), where the experimental observation shows significant discrepancy from a simple numerical model. The other is the analysis of the beam profile measurement at the exit of DTL section and SDTL (Separate-type DTL) section. In these measurements, we have observed a substantial beam quality deterioration which develops in a characteristic way. As we lack sufficient beam diagnostics in the DTL section, we have performed an IMPACT simulation to reproduce its characteristic features and then to infer its underlying mechanism.

These two topics have already been discussed in other literatures [6, 7] in detail. Then, we here try to present a brief review of these studies instead of delving into details.

## LAYOUT OF J-PARC LINAC

Before proceeding to the simulation study, we here run through the basic layout of J-PARC linac. As shown in Fig. 1, J-PARC linac consists of a 50-keV negative hydrogen ion source, 3-MeV RFQ, 50-MeV DTL, and 181-MeV SDTL. We also have a 3-m long matching section between RFQ and DTL, to which we refer as MEBT (Medium Beam Energy Transport).

MEBT consists of eight quadrupole magnets, two buncher cavities, an RF chopper system, and various beam diagnostics including four wire-scanner beam profile monitors. It also has a 45-deg bend magnet followed by a transverse emittance monitor of double-slit type.

In contrast to MEBT, the DTL section has very limited number of beam diagnostics. The DTL section consists of three DTL tanks, and its total length is 27 m. As it has no available space for beam diagnostics inside the tank, it only has a beam current monitor and a beam phase monitor at each inter-tank spacing.

In SDTL section, the quadrupole magnets are placed between tanks instead of inside the drift tube. Therefore, it has a longer inter-tank spacing which can accommodate various beam diagnostics. In particular, we have an array of four wire scanners periodically placed at the inter-tank spacings at the DTL exit (or the most upstream portion of the SDTL section). From the measurement with these wire scanners, we can calculate the transverse Twiss parameters and the rms emittance assuming a design Twiss parameters and the emittance in the longitudinal direction. We also have a similar setup at the exit of the SDTL section and some downstream locations. The SDTL section consists of 30 tanks, and its total length is about 84 m.

To be noted here is that we lack the instrumentation for longitudinal profile measurement throughout the linac, while we are planning to introduce a few bunch shape monitors of INR type [8].

## Controls and Computing

## DTL PHASE SCAN

The set-points of RF phase and amplitude for a cavity are important parameters to be determined with a beam-based tuning. To find an adequate set-point, we have performed a so-called phase scan tuning. In this tuning, the phase set-point of a cavity is scanned with a fixed amplitude while measuring the output beam energy with the TOF (Time Of Flight) method. The phase scan provides us with a dependence of the output energy on the tank phase, to which we refer as a “phase scan curve”. We iterate the same procedure with different amplitude settings, and then compare the obtained phase scan curves with a numerical model. As

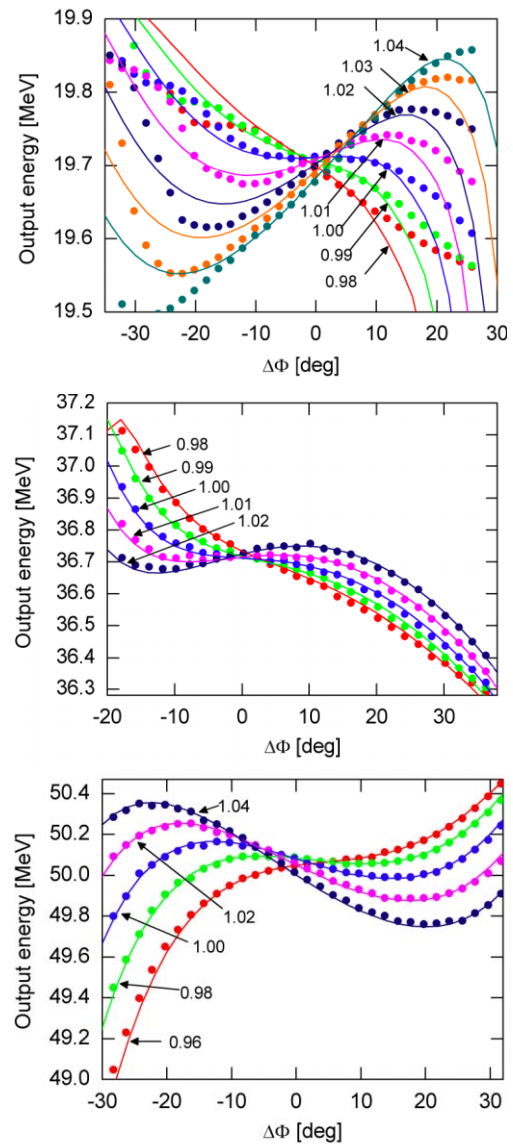


Figure 2: Measured and simulated phase scan curves for DTL1 (top), DTL2 (middle), and DTL3 (bottom). The scaled RF amplitude  $A$  is annotated for each curve. The measured results are shown with circle markers, and those from PARMILA modeling are shown with solid lines.

the phase scan curve of a DTL tank has a peculiar shape, we can find an adequate RF set-point with their signature matching. This tuning is performed one klystron at a time from the upstream end.

Figure 2 shows the phase scan result for DTL tanks, where we adopt the simple beam centroid motion simulated with PARMILA [9] as the reference for the tuning. In this figure,  $\Delta\Phi$  denotes the phase shift from the design phase setting and  $A$  is the RF amplitude scaled by its design value. It is readily seen in Fig. 2 that the measured phase scan curves are thoroughly reproduced by the numerical model for DTL2 and DTL3. However, it shows notable deviations in DTL1 especially for the case with an RF set-point away from its design value. Furthermore, the trend of the phase scan curve is totally different when the amplitude setting is lower than the design value. Even with higher amplitude, the experimental curve shows a large deviation from the modeling for a large phase shift from the design value. These disagreements prevent us from performing an accurate phase signature matching, and has motivated us to establish a more rigorous numerical model employing a fully three-dimensional multi-particle tracking.

To investigate the disagreement between the simulated beam centroid motion and the measurement for DTL1, a parallel PIC simulation has been performed with the IM-

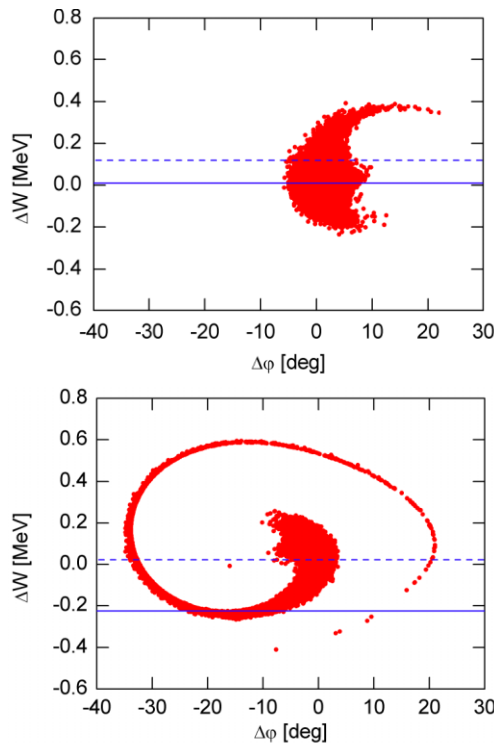


Figure 3: The longitudinal phase space distribution at the DTL1 exit simulated with the IMPACT code. Top:  $\Delta\Phi = -29.5$  deg and  $A = 1.02$ , and bottom:  $\Delta\Phi = 25$  deg and  $A = 1.00$ . The measured beam energy is shown with a broken line, and the centroid of the simulated distribution with a solid line.

## Controls and Computing

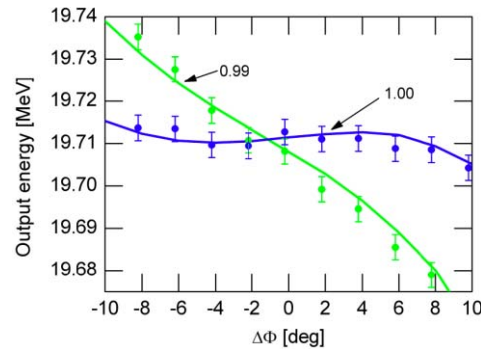


Figure 4: Measured and simulated phase scan curves for DTL1 with a restricted parameter range. Two phase scan curves are shown for  $A = 0.99$  and  $1.00$  as annotated in the figure. The measured results are shown as circle markers, and the curves from PARMILA modeling are shown with solid lines.

PACT code. The tracking is performed from the exit of the RFQ with the initial distribution obtained with the PARMTEQM [10] (which is the same with the PARMILA simulation). The nonlinear Lorentz map integrator is utilized to deal with the highly nonlinear RF force which arises from unusually large RF set-point deviations involved in the phase scan tuning. To attain a reasonable accuracy, the integration step width is set to about  $\beta\lambda/100$  with  $\beta$  and  $\lambda$  being the particle velocity scaled by the speed of light and the RF wave length, respectively. In the simulation, 95,322 simulation particles and  $32 \times 32 \times 64$  meshes are employed.

To illustrate the findings in the simulation study, we show in Fig. 3 the simulated longitudinal distribution at the DTL1 exit for two cases with  $(\Delta\Phi, A) = (-29.5$  deg,  $1.02)$  and  $(25.0$  deg,  $1.00)$ . These settings corresponds to the case where the measured phase scan curves show a significant deviation from the model. It is clearly seen in Fig. 3 that the longitudinal distribution is subject to significant filamentation with these settings. Furthermore, it has been confirmed that the extent of the filamentation is substantially dependent on the assumed initial distribution. The observed discrepancy of several tens of keV in the output energy is easily caused with a modest difference in the initial distribution. Meanwhile, we are unable to confirm the credibility of the assumed initial longitudinal distribution at the RFQ exit due to lack of longitudinal diagnostics in MEBT.

In conclusion, the discrepancy between the measured phase scan curve and that from a numerical model observed in the DTL1 tuning seems to be mainly attributable to the generation of a significant filamentation. Because the filamentation depends on the initial distribution, the discrepancy of several tens of keV is unavoidable with the RF set-point far from the design value. Then, the phase signature matching is valid only in the narrow region around the design set-point where the filamentation is sufficiently modest and insensitive to the initial distribution.

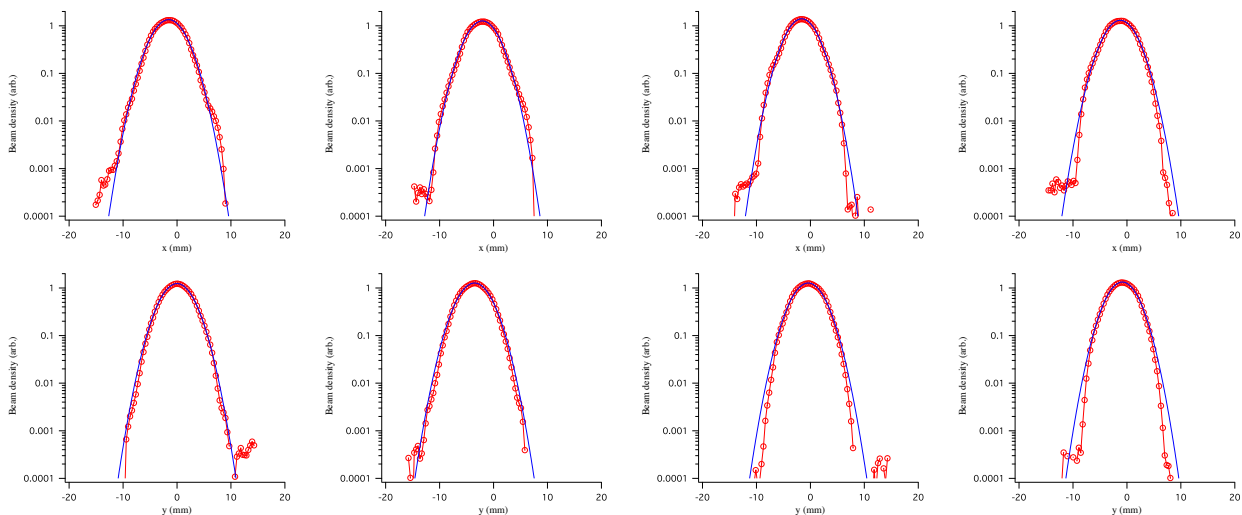


Figure 5: Typical beam profile measured at DTL exit with 30 mA peak current. Red circle: measurement, blue line: Gaussian fit. The beam profile measured with an array of four wire scanners are shown. The left two figures are the results with the first (the most upstream) wire scanner with the horizontal profile on the top and the vertical profile on the bottom. The mid-left, mid-right, and right figures are respectively results with the second, third, and fourth wire scanners. The same notation is adopted in Figs. 6, 7, and 8.

The phase scan curves for DTL1 are shown again in Fig. 7, where the parameter range is limited to have modest filamentation. It is readily seen in this figure that the experiment and the numerical model show a reasonable agreement. As seen in this figure, the goal tuning accuracy of 1 deg in phase and 1 % in amplitude is confirmed to be attainable for DTL1 with the narrow range analysis with two reference curves. It should be stressed here that the adequate phase scan range has been found with a help of the IMPACT simulation.

## BEAM PROFILE MEASUREMENT

To mitigate the beam loss in the linac and the succeeding RCS, it is practically important to suppress excess emittance growth and beam halo formation. To measure the transverse emittance and the beam tail shape, we use beam profile monitors of wire-scanner type installed along the beam line. As mentioned above, four wire scanners are periodically installed at the exit of DTL. Then, the rms emittance can be calculated from the rms beam widths measured with this wire scanner array. With the design peak current of 30 mA, the obtained rms emittance at the exit of DTL is  $0.42 \pi \text{mm}\cdot\text{mrad}$  in horizontal and  $0.36 \pi \text{mm}\cdot\text{mrad}$  in vertical. On the other hand, the measured emittance at MEBT is around  $0.22 \pi \text{mm}\cdot\text{mrad}$ . All the emittance values are normalized. These observation indicates that we have a significant emittance growth in DTL. Besides, the emittance growth is found to be modest with lower peak current of 5 mA.

We also have similar setups of wire scanners at the exit of SDTL. In the observation with these wire scanners, there is no significant emittance growth after the DTL exit in both

5-mA and 30-mA cases. This tendency has also been confirmed in more downstream sections.

Another interesting feature of the measurement is the shape of beam profile. Figure 5 shows a typical beam profile measured at the DTL exit. The beam profile is measured with four wire scanners in this section, and each wire scanner is  $7 \beta \lambda$  apart. As readily seen in this figure, the beam profile is virtually Gaussian in spite of the significant emittance growth in DTL. Contrary to our expectations, the measured beam profile at the DTL exit lacks beam halo or “shoulder-like structure”. As the phase advance between wire scanners is about 60 deg in this region, the halo is supposed to be detected by some of these wire scanners if it has been generated. Meanwhile, the halo-like structure is clearly seen at the SDTL exit as shown in Fig. 6. It should be stressed here that the halo is generated despite the absence of significant emittance growth in the SDTL section.

This interesting feature has motivated us to perform particle simulations. To reproduce the experimental result, IMPACT simulations have been performed with various mismatch conditions in MEBT. Needless to say, it is of practical importance to understand the mechanism of the emittance growth and find the way to avoid it. Especially, reduction in the transverse emittance enables more flexible painting injection into RCS, and it is expected to contribute to the beam loss mitigation in RCS.

We have performed IMPACT simulation with the same simulation conditions with those in the previous section except for the choice of integrator and its step width. We here adopt the linear map integrator with the step width of  $\beta \lambda / 10$  so that we can survey a wider parameter space.

We have tried several kinds of mismatch at MEBT artificially introduced in both of the transverse and longitudinal

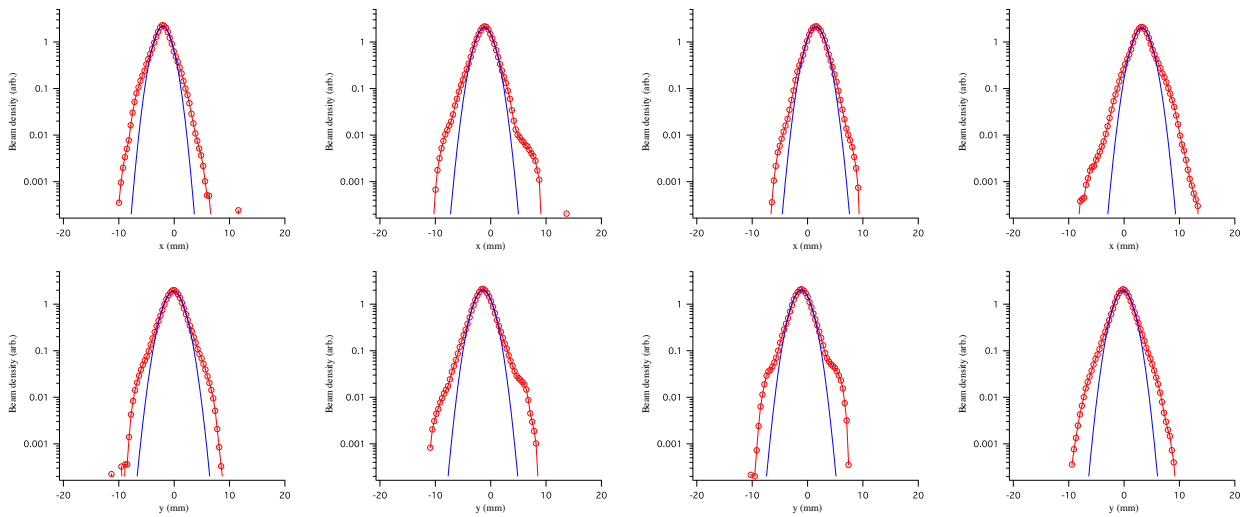


Figure 6: Typical beam profile measured at SDTL exit with 30 mA peak current.

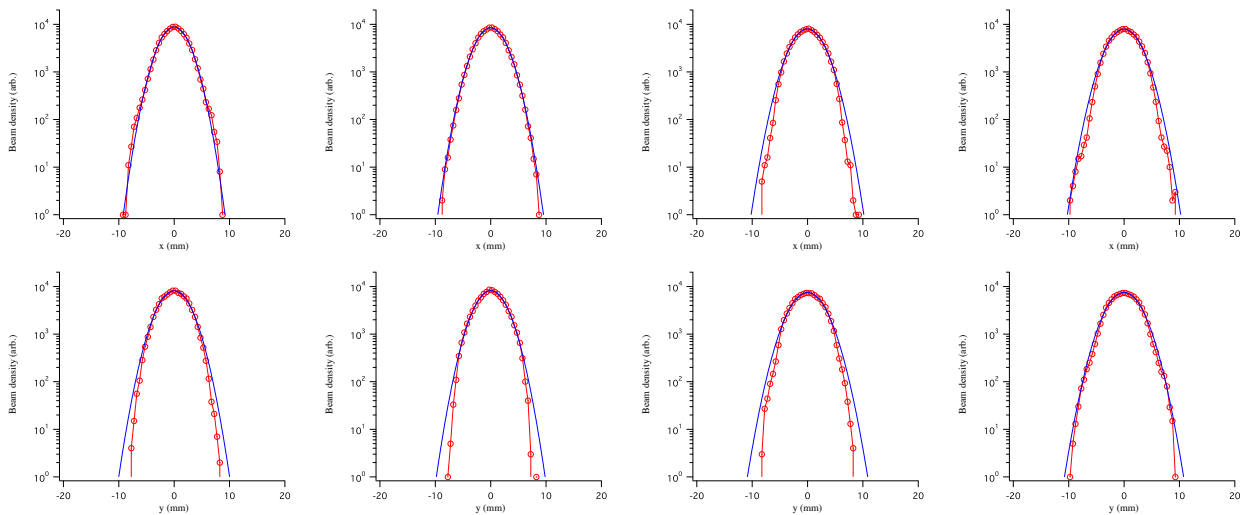


Figure 7: Simulated beam profile at DTL exit with 30 mA peak current assuming a larger longitudinal emittance than the PARMTEQ prediction.

nal directions. IMPACT simulations reveal that 30 to 40 % transverse mismatch oscillation at the upstream portion of DTL is anticipated to account for the observed emittance growth, where we define the degree of mismatch as the mismatch oscillation amplitude in the rms beam width. Either of the transverse and longitudinal mismatch in MEBT can drive the transverse mismatch oscillation in DTL through the space-charge coupling. We have also found in the simulation study that the halo develops more rapidly in most cases than the experimental observation with the assumed level of initial mismatch. In these cases, a clear halo has already been generated at the DTL exit, which disagrees with the experimental observation.

An extensive simulation study reveals that the onset of halo generation has a certain sensitivity to the kind of mismatch assumed in the simulation. Actually, the onset is

delayed in some cases with certain types of longitudinal mismatch. Figures 7 and 8 show an example of these cases, where a larger longitudinal emittance is assumed than the PARMTEQM prediction. As readily seen in these figures, the beam profile at the DTL exit is virtually Gaussian, while that at the SDTL exit has a clear halo. The emittance growth in SDTL is also confirmed to be modest in this case.

It is demonstrated in this case that the experimentally observed beam behavior can be qualitatively reproduced with a particle simulation assuming a certain type of longitudinal mismatch at MEBT. The similarity in Figs. 5, 6, 7, and 8 is significant, while the simulated halo at the SDTL exit is a little less pronounced than the measurement. This finding does not exclude the possibility that the actual cause of mismatch is different from that assumed in this case. However,

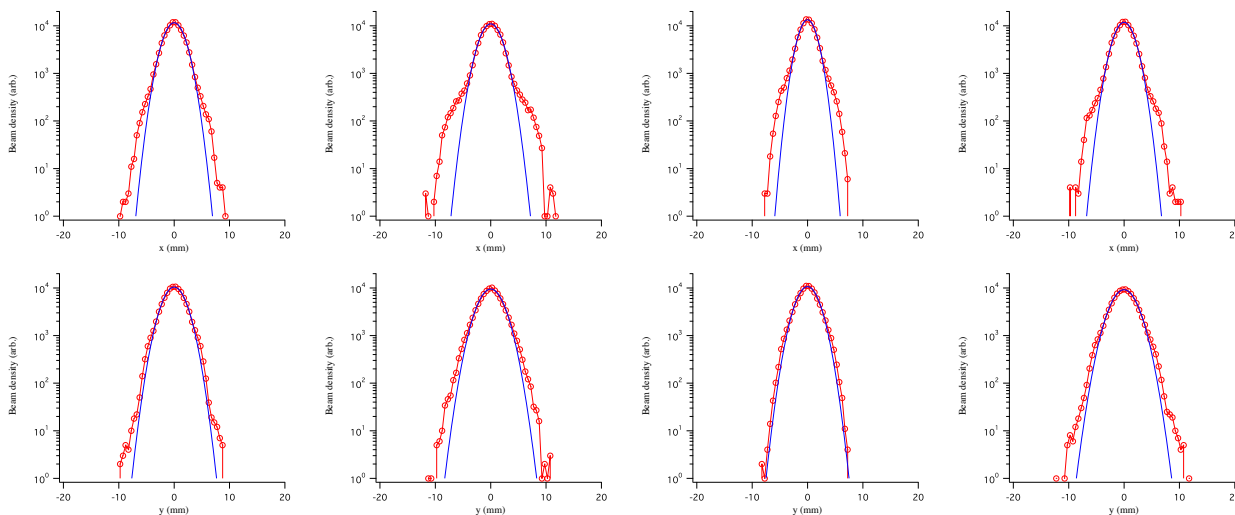


Figure 8: Simulated beam profile at SDTL exit with the same conditions as Fig. 7.

it suggests that we can narrow down the possible source of mismatch by surveying the parameter space with an extensive and comprehensive simulation. Then, it is supposed to contribute to identifying the actual cause of the mismatch utilizing the IMPACT results.

According to the observation with MEBT wire scanners, it is not likely to have a transverse mismatch of 30 to 40 % at the DTL entrance. Meanwhile, the lack of the longitudinal diagnostics at MEBT is a potential cause of excess longitudinal mismatch. These also support the hypothesis that the emittance growth is caused by a large longitudinal mismatch at MEBT. We are planning to improve the longitudinal matching in the coming beam commissioning runs by adjusting the amplitude of MEBT buncher cavities.

### SUMMARY

We have adopted the IMPACT code as an off-line model to analyze the experimental results obtained in the beam commissioning of J-PARC linac. The beams in J-PARC linac are subject to the strong space-charge forces, and various undesirable phenomena arise due to its profoundly nonlinear nature. In the beam commissioning of J-PARC linac, it is of critical importance to mitigate the uncontrolled beam loss below an extremely low level so as to secure the hands-on maintenance capability. Then, deep understanding of the space-charge-driven phenomena is essential for its beam commissioning. To this end, detailed PIC simulation is an essential tool to analyze the experimental data to help understand its underlying physics.

The experimental data obtained in the beam commissioning often fails to be comprehensive due to lack of beam diagnostics. To make up the insufficient data and to get physical understanding of it, it is often required to perform a systematic simulation study covering a wide parameter space. In this paper, we have shown two illustrative topics where the IMPACT code is used in the J-PARC linac beam

commissioning. It should be stressed here that we adopt rather modest number of simulation particles and mesh grids in these studies compared to the typical numerical study for the space-charge beam dynamics. Adopting the modest simulation condition, the IMPACT code can provide us with the simulation result in a few tens of minutes to a few years even with a multi-core PC thanks to its fully optimized feature for parallel computing. This prompt response extends the parameter space we can cover in the simulation study, and widen the possibility of realizing extremely fine tuning required for a high-power frontier machine.

### REFERENCES

- [1] M. Ikegami, "Progress in the beam commissioning of J-PARC linac and its upgrade path", to be published in Proc. of LINAC'08.
- [2] J. Galambos et. al., "XAL application programming structure", PAC'05, Knoxville, May 2005, p. 79.
- [3] H. Sako et. al., "Development of commissioning software system for J-PARC linac", PAC'07, Albuquerque, June 2007, p. 257.
- [4] J. Qiang, R. D. Ryne, S. Habib, V. Decyk, J. Comput. Phys. 163 (2000) 434.
- [5] K. R. Crandall et. al., "RFQ design codes", LA-UR-96-1836.
- [6] G. Shen, M. Ikegami, Chinese Physics C, Vol. 33 (2009), p. 577-582,
- [7] M. Ikegami, H. Sako, T. Morishita, Y. Kondo, "Measurement and simulation in J-PARC linac", to be published in Proc. of ICFA ABDW HB2008.
- [8] A. V. Feschenko, "Methods and instrumentation for bunch shape measurement", PAC'01, Chicago, June 2001, p. 517.
- [9] T. Takeda, "PARMILA", Los Alamos National Laboratory Report LA-UR-98-4487.
- [10] Y. Kondo et. al., "Particle distribution at the exit of the J-PARC RFQ", LINAC'04, Luebeck, August 2004, p. 78.